RAA 2015 Vol. **15** No. **7**, 929–938 doi: 10.1088/1674–4527/15/7/001
http://www.raa-journal.org *http://www.iop.org/journals/raa*

Research in Astronomy and Astrophysics

The broadband spectral energy distributions of SDSS blazars *

Huai-Zhen Li[1], Luo-En Chen[1], Yun-Guo Jiang[2] and Ting-Feng Yi[3]

[1] Physics Department, Yuxi Normal University, Yuxi 653100, China
[2] Shandong Provincial Key Laboratory of Optical Astronomy and Solar-Terrestrial Environment, Institute of Space Sciences, Shandong University, Weihai, 264209, China; *jiangyg@sdu.edu.cn*
[3] Physics Department, Yunnan Normal University, Kunming 650092, China

Received 2013 August 1; accepted 2015 February 13

Abstract We compiled the radio, optical and X-ray data of blazars from the Sloan Digital Sky Survey database, and presented the distribution of luminosities and broadband spectral indices. The distribution of luminosities shows that the averaged luminosity of flat spectrum radio quasars (FSRQs) is larger than that of BL Lacertae (BL Lac) objects. On the other hand, the broadband spectral energy distribution reveals that FSRQs and low energy peaked BL Lac objects have similar spectral properties, but high energy peaked BL Lac objects have a distinct spectral property. This may be due to the fact that different subclasses of blazars have different intrinsic environments and are at different cooling levels. Even so, a unified scheme is also revealed from the color-color diagram, which hints that there are similar physical processes operating in all objects under a range of intrinsic physical conditions or beaming parameters.

Key words: galaxies: active — BL Lacertae objects: general — galaxies: fundamental parameters — quasars: general

1 INTRODUCTION

Blazars are a subset of active galactic nuclei (AGNs) with strong emission at all wavelengths. They are the brightest and most variable high energy sources among AGNs, and they have continuous spectral energy distributions (SEDs). The continuum emission in blazars is thought to be from a relativistic jet oriented close to the observer and emanating from the vicinity of a black hole (Stern & Poutanen 2008; Ghisellini et al. 1986). The SEDs of blazars are characterized by a universal two-bump structure: one in the infrared to ultraviolet band, and the other in the MeV-GeV band. The synchrotron radiation in a relativistic beamed jet is responsible for the lower-energy peak, while the high-energy γ-ray emission is produced by the inverse Compton (IC) mechanism (Sambruna et al. 1996). Generally, blazars can be divided into two subclasses, BL Lacertae (BL Lac) objects and flat spectrum radio quasars (FSRQs). The main difference between these two classes is their emission lines: BL Lac objects are characterized by a lack of strong emission lines (equivalent width < 5 Å), while FSRQs have strong broad emission lines with a strength that is similar to normal quasars (Scarpa & Falomo 1997).

* Supported by the National Natural Science Foundation of China.

Based on the peak energy frequency of the synchrotron emission peak, BL Lac objects can be divided into "high energy peaked BL Lacs" (HBLs) and "low energy peaked BL Lacs" (LBLs) (Padovani & Giommi 1995; Giommi et al. 1995). Mei et al. (2002) and Ma et al. (2007) found that the two subclasses of BL Lac objects can be distinguished by their peak frequencies $\nu_{\rm peak}$: HBLs have $\log \nu_{\rm peak} > 14.7$, while LBLs have $\log \nu_{\rm peak} < 14.7$.

In addition, Padovani & Giommi (1995) found that LBLs and HBLs can also be divided by using the ratio of X-ray flux at 1 keV (in units of erg cm^{-2} s^{-1}) to 5 GHz radio flux density (in units of Janskys (Jy)). The criterion is $f_{\rm x}/f_{\rm r} \sim 10^{-11}$, corresponding to the broadband spectral index (from 5 GHz in radio to 1 keV in X-ray) $\alpha_{\rm rx} \simeq 0.75$. HBLs have a broadband spectral index of $\alpha_{\rm rx} \leq 0.75$, and LBLs have a spectral index of $\alpha_{\rm rx} > 0.75$ (Giommi et al. 1995; Ma et al. 2007; Mei et al. 2002; Urry & Padovani 1995). The SEDs of these two different subclasses of BL Lac objects have been investigated by a number of authors (e.g., Bao et al. 2008; Chen et al. 2006; Padovani & Giommi 1995; Giommi et al. 1990; Nieppola et al. 2006). Padovani & Giommi (1995) and Giommi et al. (1990) found that these two subclasses occupy different regions on the $\alpha_{\rm ro}$ - $\alpha_{\rm ox}$ plane. Padovani & Giommi (1995) also found that there are correlations between the minimum soft X-ray flux and the radio flux, and there are also correlations between the radio and optical fluxes for the subsample of HBLs but not for that of LBLs. Nieppola et al. (2006) found that there is a negative correlation between the luminosity and the synchrotron peak frequency $\nu_{\rm peak}$ at the radio and optical bands, whereas the correlation turns slightly positive in X-ray (Nieppola et al. 2006). Fan et al. (2012) and Lyu et al. (2014) found that HBLs have different properties from LBLs. Yan et al. (2014) found that the one-zone synchrotron self-Compton (SSC) model can successfully fit the SEDs of HBLs, but fails to explain the SEDs of LBLs. In addition, Bao et al. (2008) found that these two subclasses of BL Lac objects can be explained by a unified scheme.

BL Lac objects and FSRQs are grouped together under the denomination of blazars, which eliminates the somewhat ambiguous issue of the strength of emission lines as a classification criterion. However, there are some differences in the individual emission properties among different blazar subclasses. The relationship among different kinds of blazars can enhance our understanding of the fundamental properties of blazars. Therefore, it is imperative to investigate the connection among FSRQs, LBLs and HBLs.

The relationship between of BL Lac objects and FSRQs has been discussed by a number of authors (e.g., Comastri et al. 1997; Fossati et al. 1998; Ghisellini et al. 1998, 2009; Li et al. 2010; Sambruna et al. 1996; Xie et al. 2001, 2003, 2004, 2006, 2007, 2008; Zheng et al. 2007), who assembled the SED of many radio, X-ray and γ-ray selected blazars. Fossati et al. (1998) studied the SEDs of a combined blazar sample, and found that the SED properties of these subclasses present a remarkable continuity and a systematic trend as a function of source luminosity, which suggests that the parameter describing the blazar continua is likely to be the source luminosity. Based on the first Fermi sample, Ghisellini et al. (2009) found that FSRQs and BL Lac objects occupy separate regions, and obey a spectral sequence. However, Antón & Browne (2005) found that there are selection effects for the "blazar sequence" reported by Fossati et al. (1998) and Ghisellini et al. (1998). Some literature has shown that HBLs have different properties from FSRQs, but LBLs are similar to FSRQs (e.g. Chen et al. 2013; Fan et al. 2012; Li et al. 2010; Lyu et al. 2014). However, Li et al. (2010) and Chen et al. (2013) also found that their whole sample suggests there is a unified scheme of blazars. Comastri et al. (1997) discovered that there is a significant anticorrelation between X-ray and γ-ray spectral indices, and also between the broadband spectral indices $\alpha_{\rm ro}$ and $\alpha_{\rm x\gamma}$ of BL Lac objects and FSRQs. The correlation between the broadband spectral indices obtained by Comastri et al. (1997) implied that there is a different shape in the overall energy distributions from radio to γ-ray energies between BL Lac objects and FSRQs. Sambruna et al. (1996) and Xie et al. (2003) found that three kinds of blazars have different SEDs, but follow a continuous spectral sequence.

In this paper, we will study the distributions of the luminosities and the radio-optical-X-ray SEDs of SDSS blazars. We also study the connections among LBLs, HBLs and FSRQs. A detailed

explanation of the sample is given in Section 2. The distributions of luminosity are presented in Section 3. The broadband spectral energy distribution is given in Section 4. In Section 5, discussions and conclusions are presented.

2 THE SAMPLE OF SDSS BLAZARS

The Sloan Digital Sky Survey (SDSS) is one of the most ambitious and influential surveys in the history of astronomy. Plotkin et al. (2008) have drawn a large sample of 501 BL Lac object candidates from the combination of SDSS Data Release 5 (SDSS DR5) optical spectroscopy, and the Faint Images of the Radio Sky at Twenty-Centimeters (FIRST) radio survey. Plotkin et al. (2010) have presented a sample of 723 optically selected BL Lac candidates from the SDSS Data Release 7 (SDSS DR7) spectroscopic database. Based on the large radio (the NRAO VLA Sky Survey, ATCA catalogue of compact PMN sources), ROSAT All Sky Survey (RASS), the SDSS Data Release 4 (SDSS DR4) and 2dF survey data, Turriziani et al. (2007) presented a Radio-Optical-X-ray catalog compiled from at ASDC (ROXA) including 816 objects, among which 510 are confirmed blazars. In addition, Chen et al. (2009) have also presented a sample including 118 Non-thermal jet-dominated FSRQs from SDSS Data Release 3 (SDSS DR3), which is an X-ray quasar sample with the FIRST and GB6 radio catalogs. Based on the samples of Plotkin et al. (2008, 2010), Turriziani et al. (2007) and Chen et al. (2009), we compiled a large sample of 606 blazars, including 292 FSRQs and 314 BL Lacs. All the objects in the sample have matches in RASS and measured redshifts. In our sample, the three-band luminosities ($L_{\rm r}$, $L_{\rm o}$ and $L_{\rm x}$) and the broadband spectral indices $\alpha_{\rm ro}$, $\alpha_{\rm rx}$ and $\alpha_{\rm ox}$ were given in the literature (Chen et al. 2009; Plotkin et al. 2008, 2010; Turriziani et al. 2007). The luminosities $L_{\rm r}$, $L_{\rm o}$ and $L_{\rm x}$ are the specific luminosities (per unit frequency) at 5 GHz, 5000 Å and 1 keV, respectively. $\alpha_{\rm ro}$ is the two-point spectral indices between 5 GHz and 5000 Å, $\alpha_{\rm rx}$ represents the two-point spectral indices between 5 GHz and 1 keV, and $\alpha_{\rm ox}$ denotes the two-point spectral indices between 5000 Å and 1 keV.

As discussed in Section 1, BL Lac objects can be divided into HBLs and LBLs, based on the radio-X-ray spectral index $\alpha_{\rm rx}$ between 5 GHz and 1 keV. According to the literature (Giommi et al. 1995; Ma et al. 2007; Mei et al. 2002; Plotkin et al. 2008; Urry & Padovani 1995), most BL Lac objects with $\alpha_{\rm rx} \leq 0.75$ are HBLs, and most BL Lac objects with $\alpha_{\rm rx} > 0.75$ are LBLs. Therefore, to investigate the relations among different blazar subclasses, we adopt $\alpha_{\rm rx} = 0.75$ as a rough value to separate HBLs from LBLs when applied to SDSS BL Lac objects (Giommi et al. 1995; Ma et al. 2007; Mei et al. 2002; Urry & Padovani 1995). Based on this criterion, there are 270 HBLs and 44 LBLs in our sample.

3 DISTRIBUTIONS OF LUMINOSITY OF BLAZARS

Fossati et al. (1998) studied the SEDs of a combined blazar sample, and found that source luminosity is the characteristic parameter describing the blazar continua. On the basis of the first Fermi sample, Ghisellini et al. (2009) have found that BL Lac objects are harder and less luminous than FSRQs. Ghisellini et al. (1998) found that HBLs are the sources that have the lowest intrinsic power and the weakest external radiation field, LBLs are intrinsically more powerful than HBLs, and FSRQs represent the most powerful blazars.

Thus, we computed the distributions of radio (at 5 GHz), optical (at 5000 Å) and X-ray (at 1 keV) luminosities for three subclasses of blazars. Figures 1–3 show the distribution of luminosities for three kinds of blazars, and all of the luminosities are K-corrected to the source rest frame (Chen et al. 2009; Plotkin et al. 2008, 2010; Turriziani et al. 2007). The distributions of radio, optical and X-ray luminosities are plotted in Figures 1, 2 and 3, respectively.

From Figure 1, one can find that FSRQs have larger radio luminosities than BL Lac objects, while the radio luminosities of LBLs are more powerful than those of HBLs. This suggests that the radio luminosities of the three kinds of blazars, from FSRQs to LBLs to HBLs, are decreasing,

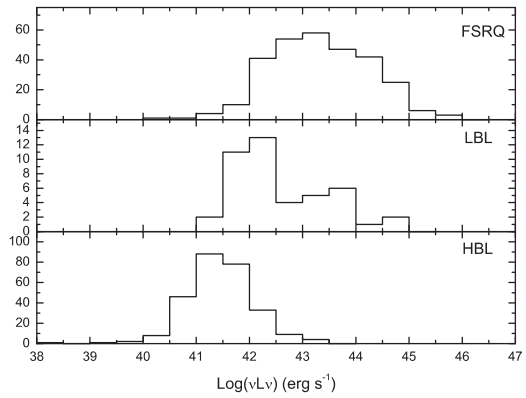

Fig. 1 Distributions of radio luminosity at 5 GHz for the three kinds of blazars used in our sample.

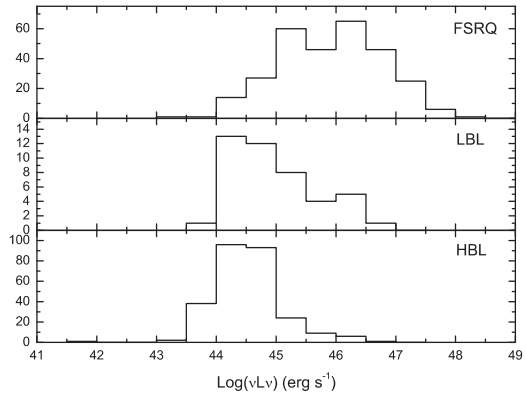

Fig. 2 Distributions of optical luminosity at 5000 Å for the three kinds of blazars used in our sample.

which is consistent with the argument reported by Ghisellini et al. (1998). In Figure 2, we can note that the optical luminosities of FSRQs are larger than those of BL Lac objects, while HBLs have similar optical luminosities to those of LBLs. Correspondingly, the X-ray luminosities of HBLs are systematically lower than FSRQs, but larger than LBLs (see Fig. 3).

The distributions presented in Figures 1, 2 and 3 show that the luminosity is an important parameter that can be used to distinguish FSRQs from BL Lac objects. A tendency of luminosities from FSRQs to BL Lac objects is revealed from the distributions of luminosities. The distributions of luminosities for three kinds of blazars presented from Figures 1–3 are consistent with the results reported by Fossati et al. (1998) and Ghisellini et al. (1998). On the other hand, one can note that all of the distributions are continuous in properties between HBLs and LBLs, as well as between FSRQs and BL Lac objects, which is in good agreement with the previous arguments about the continuum of blazars (Fossati et al. 1998; Ghisellini et al. 1998; Xie et al. 2003; Comastri et al. 1997; Sambruna et al. 1996).

4 BROADBAND SPECTRAL ENERGY DISTRIBUTION OF BLAZARS

Searching for the connection among different blazar subclasses is very significant because it can substantially enhance our understanding of the fundamental nature of blazars. The relationship among

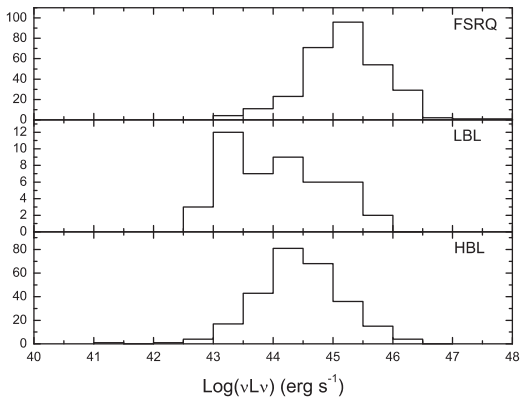

Fig. 3 Distributions of X-ray luminosity at 1 keV for the three kinds of blazars used in our sample.

different blazars has been discussed in the literature with a unified scheme and a spectral sequence for blazars (Fossati et al. 1998; Ghisellini et al. 1998; Sambruna et al. 1996; Xie et al. 2003). For investigating the relationship among different subclasses of blazars, we will analyze the relationship among the HBLs, LBLs and FSRQs on the basis of the broadband spectral indices $\alpha_{\rm ro}$, $\alpha_{\rm rx}$ and $\alpha_{\rm ox}$.

4.1 Diagram of $\alpha_{\rm rx}$ versus $\alpha_{\rm ro}$

Here, we investigate the relationship between the broadband spectral indices $\alpha_{\rm rx}$ and $\alpha_{\rm ro}$ for the whole sample. The plot is shown in Figure 4. Figure 4 shows that there is a good correlation between $\alpha_{\rm rx}$ and $\alpha_{\rm ro}$ for the whole sample. An equation derived by linear regression analysis for all of the samples is written as

$$\alpha_{\rm rx} = (0.64 \pm 0.03)\alpha_{\rm ro} + (0.43 \pm 0.01), \quad (1)$$

with a correlation coefficient of $r = 0.70$ and a chance probability of $p < 10^{-4}$. Moreover, we also study the relationship between $\alpha_{\rm rx}$ and $\alpha_{\rm ro}$ for the FSRQs and LBLs sample. We obtain

$$\alpha_{\rm rx} = (0.42 \pm 0.02)\alpha_{\rm ro} + (0.59 \pm 0.01), \quad (2)$$

with a correlation coefficient of $r = 0.70$ and a chance probability of $p < 10^{-4}$. The correlation analysis suggests that there is a linear correlation between $\alpha_{\rm rx}$ and $\alpha_{\rm ro}$ for the whole sample, as well as for the FSRQs+LBLs sample. This provides evidence for the unified scheme reported by Fossati et al. (1998) and Ghisellini et al. (1998).

In addition, Figure 4 shows that the majority of FSRQs and LBLs are mixed together, which suggests that they have similar spectral properties. However, Figure 4 also reveals that the distribution of HBLs in the $\alpha_{\rm rx}$ versus $\alpha_{\rm ro}$ diagram is different from that of FSRQs and LBLs. This indicates that HBLs have different spectral properties from FSRQs and LBLs. These results are consistent with the reported results of Xie et al. (2003), who found that HBLs and LBLs are located in different regions in the $\alpha_{\rm ox} - \alpha_{\rm x\gamma}$ plane, but that the LBLs and FSRQs occupy the same region in the $\alpha_{\rm ox} - \alpha_{\rm x\gamma}$ plane. In addition, our results also agree with those reported by Fan et al. (2012) and Lyu et al. (2014).

4.2 Diagram of $\alpha_{\rm rx}$ versus $\alpha_{\rm ox}$

In Figure 5, $\alpha_{\rm rx}$ versus $\alpha_{\rm ox}$ is plotted for our SDSS blazar sample. We can find that the distribution of three kinds of blazars revealed from Figure 5 is similar to that of Figure 4. For the whole sample, Figure 5 shows a significant correlation between $\alpha_{\rm rx}$ and $\alpha_{\rm ox}$, and the linear regression

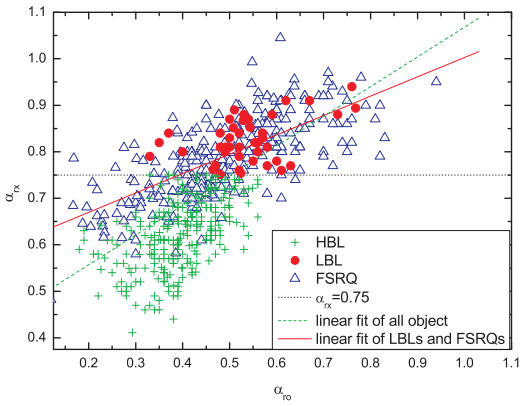

Fig. 4 The relationship between the broadband spectral indices $\alpha_{\rm ro}$ and $\alpha_{\rm rx}$ for the sources in our sample.

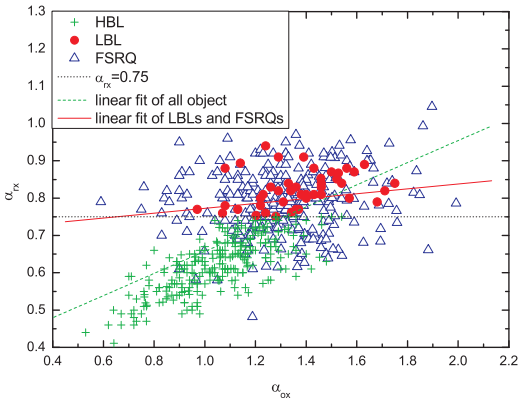

Fig. 5 The relationship between the broadband spectral indices $\alpha_{\rm ox}$ and $\alpha_{\rm rx}$ for the sources in our sample.

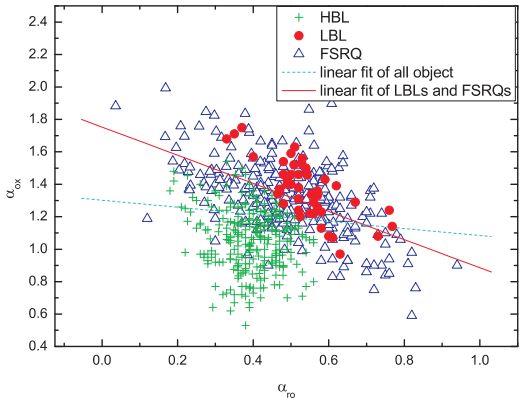

Fig. 6 The relationship between the broadband spectral indices $\alpha_{\rm ro}$ and $\alpha_{\rm ox}$ for the sources in our sample.

analysis yields

$$\alpha_{\rm rx} = (0.30 \pm 0.01)\alpha_{\rm ox} + (0.36 \pm 0.02), \tag{3}$$

with a correlation coefficient of $r = 0.62$ and a chance probability of $p < 10^{-4}$. Moreover, Figure 5 shows that there is a weak correlation between $\alpha_{\rm rx}$ and $\alpha_{\rm ox}$ for the FSRQs and LBLs sample, and the linear regression analysis produces equation

$$\alpha_{\rm rx} = (0.07 \pm 0.02)\alpha_{\rm ox} + (0.71 \pm 0.03), \tag{4}$$

with a correlation coefficient of $r = 0.17$ and a chance probability of $p = 0.0016$. In Figure 5, one can note that the majority of FSRQs and LBLs also occupy the same region, but the HBLs occupy a separate distinct region, which is also consistent with the previous results.

4.3 Diagram of $\alpha_{\rm ox}$ versus $\alpha_{\rm ro}$

Based on the broadband spectral index $\alpha_{\rm ox}$ versus $\alpha_{\rm ro}$, we investigate the relationships between $\alpha_{\rm ox}$ and $\alpha_{\rm ro}$. Figure 6 plots $\alpha_{\rm ox}$ versus $\alpha_{\rm ro}$. A linear regression analysis shows that there is a weak or

even no correlation between $\alpha_{\rm ox}$ and $\alpha_{\rm ro}$ ($r = -0.11$ and $p = 0.054$) for the whole sample. This independent relation is obviously inconsistent with the foregoing correlation revealed from Figure 4 and Figure 5. However, the correlation is significant when considering the FSRQs and LBLs sample, and the linear regression analysis equation is

$$\alpha_{\rm ox} = (0.87 \pm 0.07)\alpha_{\rm ro} + (1.75 \pm 0.04), \quad (5)$$

where the correlation coefficient is $r = -0.56$ and the chance probability is $p < 10^{-4}$. This suggests that the HBLs are different from FSRQs, but LBLs are similar to FSRQs. In addition, Figure 6 also shows that most of the FSRQs and LBLs are located in the same region in the $\alpha_{\rm ox}$ -$\alpha_{\rm ro}$ plot, but the HBLs occupy a separate distinct region in the $\alpha_{\rm ox}$ versus $\alpha_{\rm ro}$ plane. This is consistent with the distribution shown in Figure 4 and Figure 5. This supports the foregoing results: FSRQs and LBLs have similar spectral properties, but the HBLs have distinct spectral properties.

4.4 Summary

As noted above, from Figures 4 and 5, there is a strong correlation between $\alpha_{\rm rx}$ and $\alpha_{\rm ro}$, as well as between $\alpha_{\rm rx}$ versus $\alpha_{\rm ox}$ for the whole sample, which provides some more evidence for the conclusion reported by Fossati et al. (1998) and Ghisellini et al. (1998); namely, there is a unified scheme for blazars. On the other hand, from Figures 4, 5 and 6, one can note that there are also some different distributions from the blazar sequence reported by Fossati et al. (1998) and Ghisellini et al. (1998). In the color-color diagram, HBLs and FSRQs occupy separate regions, while the LBLs and FSRQs are mixed together, which is consistent with what is reported in some literature (e.g. Chen et al. 2013; Fan et al. 2012; Li et al. 2010; Lyu et al. 2014; Xie et al. 2003). This suggests that FSRQs and LBLs have similar properties, but HBLs have distinct properties.

5 DISCUSSION AND CONCLUSIONS

Based on the Slew Survey, the 1 Jy samples of BL Lacs and the 2 Jy sample of FSRQs, Fossati et al. (1998) studied the systematics of the SEDs of blazars using data from the radio to the γ-ray band, and found that three different kinds of blazars follow an almost continuous spectral sequence: from FSRQs through LBLs to HBLs. Ghisellini & Tavecchio (2008) revisited the so called "blazar sequence," and proposed that the power of the jet and the SED of its emission are linked to the two main parameters of the accretion process. A similar trend was also obtained by other authors (e.g. Xie et al. 2003; Sambruna et al. 1996; Ghisellini et al. 1998; Böttcher & Dermer 2002; Maraschi et al. 2008) who found that similar physical processes operate in three kinds of blazars. However, Antón & Browne (2005) found that there are selection effects for the "blazars sequence." Moreover, some authors have found that HBLs do not follow the blazar sequence (e.g. Chen et al. 2013; Fan et al. 2012; Giommi et al. 2005; Li et al. 2010; Padovani et al. 2003; Padovani 2007) .

In this paper, we computed the distributions of the radio (at 5 GHz), optical (at 5000 Å) and X-ray (at 1 keV) luminosities. The distributions of luminosities reveal that luminosity is both an important parameter to distinguish FSRQs from BL Lac objects and the distributions are continuous for the three kinds of blazars. The luminosities of FSRQs are larger than those of BL Lac objects, which is in good agreement with the arguments reported by other authors (Abdo et al. 2009; Fossati et al. 1998; Ghisellini et al. 1998; Sambruna et al. 1996). The distributions of radio luminosity support the blazar sequence reported by Fossati et al. (1998) and Ghisellini et al. (1998). However, the distributions of optical and X-ray luminosities do not support this sequence.

The broadband energy distribution shows that three kinds of blazars have different spectral properties. It also shows that most FSRQs and LBLs are mixed together in the color-color diagram (see Figs. 4, 5 and 6), which is consistent with previous results (Fan et al. 2012; Li et al. 2010; Sambruna et al. 1996; Xie et al. 2003; Zheng et al. 2007). This suggests that they have similar spectral properties, which provide more evidence for the conclusion of the unified scheme. However, the location of

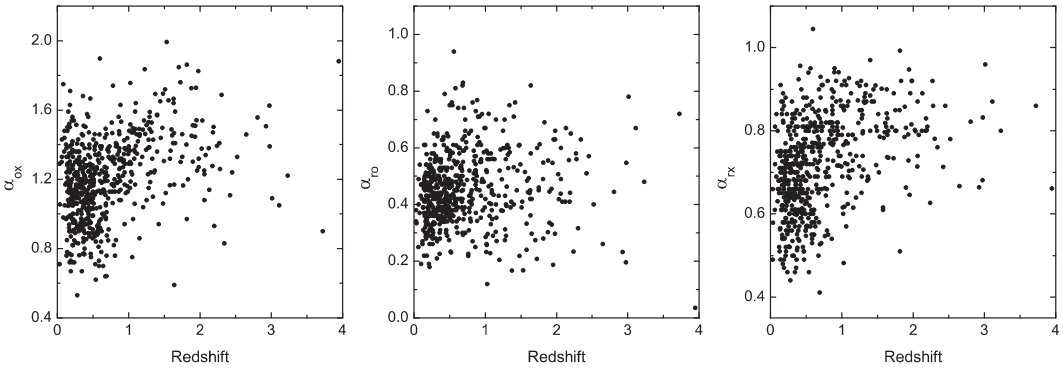

Fig. 7 Relations between redshift and spectral indices.

HBLs is separate from that of FSRQs and LBLs in the color-color diagram, which reveals that HBLs have different SEDs from FSRQs and LBLs. This suggests that the results from the SDSS sample do not support the so called "blazar sequence," which is consistent with the results reported by other authors (Antón & Browne 2005; Fan et al. 2012; Chen et al. 2013; Li et al. 2010; Padovani et al. 2003; Padovani 2007; Zhang et al. 2013). The spectral sequence obtained by Fossati et al. (1998) may be related to the selection effects, because the samples used by Fossati et al. (1998) are classic, high flux limited surveys in the radio and X-ray (Antón & Browne 2005). The sample that we used in this paper is a large sample that includes 606 blazars, which can provide an unbiased view of the spectral properties of quasars. Moreover, Figure 7 plots the relations between the redshift and spectral indices. Figure 7 shows that the spectral indices are independent of redshift, which suggests that the selection effects in our sample are weak.

Ghisellini et al. (1998) suggested the level of cooling is different for different subclasses of blazars. FSRQs suffer stronger cooling and synchrotron emission peaks at a much lower frequency. However, the cooling is less important for HBLs, and the energetic particles can produce synchrotron and IC emissions up to high frequency. The level of cooling in FSRQs is stronger than that of HBLs, which may be due to the external radiation field (Ghisellini et al. 1998). Georganopoulos et al. (2001) suggested that the radiating jet plasma in weak sources is outside the broad line scattering region (BLR), but it is within in the power source. This implies that the location of the emitting region between HBLs and FSRQs might be very different (Costamante 2009). The jet energy of FSRQs would dissipate within the BLR, leading the high energy electrons in the jet to suffer greater cooling (Chen & Bai 2011). Ghisellini et al. (2010) suggested that the γ-ray emission from FSRQs is likely from the Compton scattering of an external radiation source, while for HBLs the SSC is able to provide a good fit to the γ-ray emission. In addition, based on the physical properties of relativistic jets, Yan et al. (2014) found that the one-zone SSC model can successfully fit the SEDs of HBLs, but fails to explain the SEDs of LBLs. Moreover, they also suggest that the ratios of the Compton to the synchrotron peak energy fluxes of LBLs are greater than those of HBLs and LBLs, and then LBLs are Compton dominated (Yan et al. 2014). This suggests that there is an external radiation field for LBLs. Therefore, the levels of cooling of FSRQs and LBLs are stronger than those of HBLs, which leads us to conclude the synchrotron emission peaks of FSRQs and LBLs are lower than those of HBLs. Abdo et al. (2010) found FSRQs and LBLs are low synchrotron peaked blazars, while HBLs are high synchrotron peaked blazars. Fan et al. (2012) suggested that if the synchrotron peak frequency moves to a lower frequency, then the IC peak frequency may also move to a lower frequency. Thus, the X-rays produced by LBLs and FSRQs come from the combination of synchrotron emission and the IC emission, while the X-rays generated by HBLs come from the synchrotron emission of very high energy electrons (Abdo et al. 2010; Fan et al. 2012). In addition, the different SEDs between HBLs, FSRQs and LBLs may be related to the different intrinsical

environments around the blazar's nucleus. The intrinsical environments of FSRQs and HBLs have a clear physical difference: the environment of HBLs is "cleaner" than that of FSRQs (Costamante 2009). The central regions of FSRQs are rich in gas and dust, which leads to a higher accretion rate onto the central supermassive black hole (Böttcher & Dermer 2002). Moreover, the material would efficiently reprocess and scatter radiation from the accretion disk. This would lead to the observed strong optical emission lines in the BLR and to a high energy density of the external soft-photon field in the jet (Böttcher & Dermer 2002).

Although HBLs have different SEDs from FSRQs and LBLs, the significant correlation revealed from Figures 4 and 5 suggests that there is a unified scheme for the whole sample, which is consistent with the previous conclusion reported by other authors (Comastri et al. 1997; Fossati et al. 1998; Ghisellini et al. 1998; Li et al. 2010; Sambruna et al. 1996; Xie et al. 2001, 2003). This hints that there are similar physical processes operating in all these objects. In the case of the blazar-type sources where the emission is usually associated with a stream from a relativistic jet, the overall spectrum is determined by the energy spectrum of the electrons as well as by the variation of physical quantities along the jet (Begelman et al. 1984). HBLs, LBLs and FSRQs have a significant correlation in the color-color diagram (see Figs. 4 and 5), which implies that similar physical processes operate in all objects under a range of intrinsic physical conditions or beaming parameters. On the other hand, the difference among three subclasses of blazars, as revealed from the color-color diagram (see Figs. 4, 5 and 6), could be attributed to the different levels of cooling and the intrinsically different environments around the blazars' nucleus for different subclasses of blazars, which leads to different optical and X-ray spectra for different kinds of blazars.

Acknowledgements We are grateful to the anonymous referee for useful comments. We are grateful for help from Liang Chen. This research has made use of the SDSS database. This work is supported by the National Natural Science Foundation of China (NSFC, No. 10878013), the Natural Science Foundation of Yunnan Province (2011FZ081, 2012FD055 and 2013FB063), the Program for Innovative Research Team (in Science and Technology) in University of Yunnan Province (IRTSTYN), the Science Research Foundation of Yunnan Education Department of China (2012Y316), and the Young Teachers Program of Yuxi Normal University. In addition, the work of Yunguo Jiang is supported by the NSFC under Grant No. 11403015.

References

Abdo, A. A., Ackermann, M., Ajello, M., et al. 2009, ApJ, 700, 597
Abdo, A. A., Ackermann, M., Agudo, I., et al. 2010, ApJ, 716, 30
Antón, S., & Browne, I. W. A. 2005, MNRAS, 356, 225
Bao, Y., Chen, L., Li, H., et al. 2008, Ap&SS, 318, 169
Begelman, M. C., Blandford, R. D., & Rees, M. J. 1984, Reviews of Modern Physics, 56, 255
Böttcher, M., & Dermer, C. D. 2002, ApJ, 564, 86
Chen, L., & Bai, J. M. 2011, ApJ, 735, 108
Chen, L. E., Li, H. Z., Yi, T. F., Zhou, S. B., & Li, K. Y. 2013, RAA (Research in Astronomy and Astrophysics), 13, 5
Chen, L. E., Xie, G. Z., Ren, J. Y., Zhou, S. B., & Ma, L. 2006, ApJ, 637, 711
Chen, Z., Gu, M., & Cao, X. 2009, MNRAS, 397, 1713
Comastri, A., Fossati, G., Ghisellini, G., & Molendi, S. 1997, ApJ, 480, 534
Costamante, L. 2009, International Journal of Modern Physics D, 18, 1483
Fan, J. H., Yang, J. H., Yuan, Y. H., Wang, J., & Gao, Y. 2012, ApJ, 761, 125
Fossati, G., Maraschi, L., Celotti, A., Comastri, A., & Ghisellini, G. 1998, MNRAS, 299, 433
Georganopoulos, M., Kirk, J. G., & Mastichiadis, A. 2001, in Astronomical Society of the Pacific Conference Series, 227, Blazar Demographics and Physics, eds. P. Padovani, & C. M. Urry, 116

Ghisellini, G., Maraschi, L., Treves, A., & Tanzi, E. G. 1986, ApJ, 310, 317
Ghisellini, G., Celotti, A., Fossati, G., Maraschi, L., & Comastri, A. 1998, MNRAS, 301, 451
Ghisellini, G., & Tavecchio, F. 2008, MNRAS, 387, 1669
Ghisellini, G., Maraschi, L., & Tavecchio, F. 2009, MNRAS, 396, L105
Ghisellini, G., Tavecchio, F., Foschini, L., et al. 2010, MNRAS, 402, 497
Giommi, P., Barr, P., Pollock, A. M. T., Garilli, B., & Maccagni, D. 1990, ApJ, 356, 432
Giommi, P., Ansari, S. G., & Micol, A. 1995, A&AS, 109, 267
Giommi, P., Piranomonte, S., Perri, M., & Padovani, P. 2005, A&A, 434, 385
Li, H. Z., Xie, G. Z., Yi, T. F., Chen, L. E., & Dai, H. 2010, ApJ, 709, 1407
Lyu, F., Liang, E. W., Liang, Y. F., et al. 2014, ApJ, 793, 36
Ma, L., Chen, L. E., Xie, G. Z., et al. 2007, ChJAA (Chin. J. Astron. Astrophys.), 7, 345
Maraschi, L., Foschini, L., Ghisellini, G., Tavecchio, F., & Sambruna, R. M. 2008, MNRAS, 391, 1981
Mei, D. C., Zhang, L., & Jiang, Z. J. 2002, A&A, 391, 917
Nieppola, E., Tornikoski, M., & Valtaoja, E. 2006, A&A, 445, 441
Padovani, P. 2007, Ap&SS, 309, 63
Padovani, P., & Giommi, P. 1995, MNRAS, 277, 1477
Padovani, P., Perlman, E. S., Landt, H., Giommi, P., & Perri, M. 2003, ApJ, 588, 128
Plotkin, R. M., Anderson, S. F., Hall, P. B., et al. 2008, AJ, 135, 2453
Plotkin, R. M., Anderson, S. F., Brandt, W. N., et al. 2010, AJ, 139, 390
Sambruna, R. M., Maraschi, L., & Urry, C. M. 1996, ApJ, 463, 444
Scarpa, R., & Falomo, R. 1997, A&A, 325, 109
Stern, B. E., & Poutanen, J. 2008, MNRAS, 383, 1695
Turriziani, S., Cavazzuti, E., & Giommi, P. 2007, A&A, 472, 699
Urry, C. M., & Padovani, P. 1995, PASP, 107, 803
Xie, G., Dai, B., Liang, E., Ma, L., & Jiang, Z. 2001, PASJ, 53, 469
Xie, G. Z., Dai, H., Mao, L. S., et al. 2006, AJ, 131, 1210
Xie, G. Z., Ding, S. X., Dai, H., Liang, E. W., & Liu, H. T. 2003, International Journal of Modern Physics D, 12, 781
Xie, G. Z., Zhou, S. B., & Liang, E. W. 2004, AJ, 127, 53
Xie, Z. H., Dai, H., Hao, J. M., Du, L. M., & Zhang, X. 2007, ChJAA (Chin. J. Astron. Astrophys.), 7, 209
Xie, Z. H., Hao, J. M., Du, L. M., Zhang, X., & Jia, Z. L. 2008, PASP, 120, 477
Yan, D., Zeng, H., & Zhang, L. 2014, MNRAS, 439, 2933
Zhang, J., Zhang, S. N., & Liang, E. W. 2013, International Journal of Modern Physics Conference Series, 23, 54
Zheng, Y. G., Zhang, X., & Hu, S. M. 2007, Ap&SS, 310, 1